J. Water Environ. Nanotechnol., 3(2): 116-127 Spring 2018

ORIGINAL RESEARCH PAPER

Photocatalytic degradation of organic dyes pollutants in the industrial textile wastewater by using synthesized TiO_2, C-doped TiO_2, S-doped TiO_2 and C,S co-doped TiO_2 nanoparticles

Elsayed Talat Helmy[1], Ahmed El Nemr[1]*, Mahmoud Mousa[2], Esam Arafa[3], Shady Eldafrawy[3]

[1]Environment Division, National Institute of Oceanography and Fisheries, Kayet Bey, Elanfoushy, Alexandria, Egypt
[2]Chemistry Department, Faculty of Science, Benha University, Cairo, Egypt
[3]Chemistry Department, Faculty of Science, Mansoura University, 35516-Mansoura, Egypt

Received: 2017.11.06 Accepted: 2018.01.20 Published: 2018.04.30

ABSTRACT
This paper describes the photocatalytic degradation of Reactive Blue 19 (RB-19) and Reactive Red 76 (RR-76) dyes pollutant in the industrial wastewater using TiO_2, C-doped TiO_2 (C-TiO_2), S-doped TiO_2 (S-TiO_2) and C,S co-doped TiO_2 (C,S-TiO_2) nanoparticles as photocatalysts, which were synthesized via sol-gel process. The prepared photocatalysts were characterized by scanning electron microscopy (SEM), X-Ray diffraction (XRD), Fourier transformer infra-red spectroscopy (FTIR), Energy dispersive spectroscopy (EDAX) and ultraviolet-visible absorption spectroscopy (UV-Vis). The dyes degradation was investigated under several experimental parameters such as pH, catalyst load, dye concentration, shaking speed, irradiation time and catalyst recovery. The photocatalytic dose was found to be 1.6 g/L and the efficiency of RB-19 and RR-76 photocatalytic degradation attained 100 % after 1 h irradiation time under visible light. The chemical oxygen demand (COD) values were determined for wastewater and treated wastewater. Toxicity and biological activity of the treated and untreated wastewater on marine aquatic organisms rotifer, artemia and *Vibrio parahaemolyticus* were investigated.

Keywords: *Non-Metal Doped Tio_2 Nps; Photocatalytic Degradation; Reactive Blue 19 Dye; Reactive Red 76 Dye; Sol-Gel Process*

How to cite this article
Helmy ET, El Nemr A, Mousa M, Arafa E, Eldafrawy, S. Photocatalytic degradation of organic dyes pollutants in the industrial textile wastewater by using synthesized TiO_2, C-doped TiO_2, S-doped TiO_2 and C,S co-doped TiO_2 nanoparticles . J. Water Environ. Nanotechnol., 2018; 3(2): 116-127. DOI: 10.22090/jwent.2018.02.003

INTRODUCTION

Monitoring and controlling of many natural and synthetic pollutants are very difficult, although they are known or suspected to cause harmful ecological effects and can be deleterious to human health [1]. There are large amounts of organic load in textile wastewater which cause harmful effects to the surrounding environment and human life. In the industries of textile there is more interest for the processed water. Since the treated wastewater in the textile industry is required to reach strict quality standards before reuse becomes possible, advanced techniques of purification must be available, which should be efficient and reliable [2]. Treatment of wastewater for recycling means an additional cost in manufacturing for products. It can become economically available if it brings about reduced

* Corresponding Author Email: *ahmedmoustafaelnemr@yahoo.com*
ahmed.m.elnemr@gmail.com

water intake costs and decreases discharge fees. Textile dyes and other industrial dye stuffs contain one of the largest groups of organic compounds that cause an increasing environmental danger. Up to 20% of dyes total world production is lost during the dyeing process and is released into the textile effluents [3, 4]. Even at very low concentrations some dyes are toxic and may significantly affect aquatic life and some other dyes may cause skin irritation, allergy and cancer to humans [5, 6]. Most of the conventional methods of treatment are not designed to remove trace organic contaminants and relatively high amounts of these pollutants and their metabolites can reach the aquatic environment via effluents.

Several works appeared on the photocatalytic degradation properties of pure and doped TiO_2 and TiO_2/AC using Methyl orange (MO), Rhodamine B (RhB) or acid fuchsine (AF) as model of dye compounds [7-13]. The morphological influence of TiO_2 nanostructures on photocatalytic degradation of different organic dyes has been reported [14]. N-doped TiO_2 nanoparticles caged in MIL-100(Fe) as efficient photocatalyst was investigated [15]. Biphasic TiO_2 nanoparticles decorated graphene nanosheets for photocatalytic degradation of organic dyes was reported [16]. Degradation method using light provides economically and satisfactory viable solutions in the decomposition of organic pollutants as well as harmful bacteria in the aqueous medium [17-19]. The degradation method is fast, effective, eco-friendly, economically viable and efficient in the treatment of wastewater. Also, advanced oxidation process has been used as an effective degradation method of textile wastewater [20-22]. The main objective of this research is to investigate the comparative photocatalytic degradation of synthesized C-TiO_2, S-TiO_2 and C,S-TiO_2 nanoparticles (NPs), using sol-gel method, in visible light range. The prepared NPs were characterized by scanning electron microscopy (SEM), X-Ray diffraction (XRD), Fourier transform infra-red spectroscopy (FTIR), Energy dispersive spectroscopy (EDAX) and ultraviolet-visible absorption spectroscopy (UV-Vis). The photocatalytic degradation of organic dyes pollutants (RB-19) and (RR-76) present in the industrial wastewater was investigated under several experimental parameters. Namely pH, catalyst load, dye concentration, irradiation time, shaking speed and catalyst recovery were assessed to establish the optimum operating conditions. Furthermore, to ensure the validity of degradation process, toxicity of treated and untreated wastewater on marine organism rotifer and artemia was also investigated.

MATERIALS AND METHODS

Collection and processing of industrial dye wastewater sample

Industrial dye wastewater sample was collected from the drain source of El-Mesairy company for textile spinning, weaving and dyeing, El-Mahla, El-Gharbia State, Egypt during April 2016. Wastewater was used directly without any purification. The collected wastewater was stored in a tightly closed brown glass bottle to protect it from sunlight and left in refrigerator until used.

Synthesis of nanoparticles

Titanium (IV) isopropoxide was purchased from Sigma Aldrich, glucose mono hydrate and thiourea from Fluka, and Nutrient agar from OXOID L.T.D., Basingstoke, and Hampshire, England. 5 ml of titanium(IV) isopropoxide was added to 50 ml of 1-butanol with magnetic stirring at 50 °C for 30 minutes, then pH was adjusted to 8-9 using 0.1N of NaOH solution; the solution was kept at magnetic stirrer for 2 hours, left to age for 24 h at 50 °C in oven (Lenton WF120, UK), then filtered, washed with water, 1-butanol and ethanol, dried, grinded and thermally pretreated in a muffle furnace (Naberthrm GmbH, Germany) at 400 °C for 3 h in air. While for prepared other non-metals doped TiO_2, the same procedure was used with adding appropriate amounts of carbon and sulphur (19% C, 3.54% S and 19%, 3% C,S, respectively) precursors. Glucose mono hydrate and thiourea were used as sources of C and S doped materials, respectively.

Samples Characterization

Morphological structure of prepared samples was analysed by scanning electron microscopy (SEM) (JEOL JEM-100CX II, accelerating voltage 25 kV), (FT-IR Platinum ATR-Bruker Optics) was used to analyse FT-IR spectra of the samples at a range of 400-4000 cm^{-1} and the X-ray diffraction (XRD) patterns of the samples were measured at room temperature using Rigaku D/MAX 2500 X-ray diffractometer (CuK$\alpha\lambda$ = 0.154 nm) radiation under 40 kV and 100 mA. UV-Vis absorption spectra of the samples was recorded with a Unicam V_2-30 UV-Vis spectrophotometer. Toxicity of treated and untreated wastewater was observed under microscope (*Nikon* Eclipse *200*

LED Trinocular *Microscope provided with Nikon* DSLR *camera, japan).*

Evaluation of photocatalytic activity

The photocatalytic activities of the samples were evaluated by the degradation of (RB-19) and (RR-76) in a cylindrical flask in a shaking incubator in response to visible light. A typical experiment was performed as follows: in a 100 mL vessel, different doses of catalyst (0.010, 0.020, 0.040, 0.080 and 0.16 g) of the samples were dispersed in 50 mL of collected wastewater solution. Before illumination, the mixtures were magnetically stirred in the dark to ensure the establishment of adsorption/desorption equilibrium of RB-19 and RR-76 on the sample surfaces. Subsequently, the mixtures were irradiated with 400 W halide lamp which is used as visible light source. The distance between the lamp and the aqueous suspension was kept at 15 cm. At given intervals, 3 mL of the suspension was sampled and subsequently centrifuged at a rate of 200 rpm for 10 min to remove the particles of catalyst. The absorbance of RB-19 and RR-76 was determined at 592 nm and 542 nm, respectively, using Analytik Jena General TU-1300 UV-vis spectrophotometer. The dye concentrations in wastewater were determined from a calibration curve produced between the absorbance and the concentration of dye. The organic dyes pollutants photocatalytic degradation was investigated under several experimental parameters such as pH, catalyst load, organic concentration, irradiation time, shaking speed and catalyst recovery.

Determination of chemical oxygen demand

The maximum reduction of carbon content in the wastewater and treated wastewater was determined using closed reflux standard titrimetric method. Based on the COD results, the photocatalytic degradation efficiency was calculated [23] by the following Equation (1)

$$\eta = \frac{COD_i - COD_T}{COD_i} \times 100 \quad (1)$$

Where η is photocatalytic degradation efficiency, COD_i is chemical oxygen demand of untreated wastewater and COD_T is chemical oxygen demand of treated wastewater.

Toxicity

The toxicity of untreated and treated wastewater solutions through bioassays was monitored for the catalysts used in this study. The whole sample toxicity was determined according to standard USEPA [24]. All samples were tested without dilution. Untreated initial wastewater solutions were tested as a reference for each series of toxicity tests on a daily basis, negative test (distilled water, <5% of toxicity) is in the acceptable range.

Artemia salina

Artemia cysts (RAC) (AF/N2000) were obtained from the Invertebrates Department, National Institute of Oceanography and Fisheries (NIOF), Alexandria, Egypt. The activation of cysts occurred in a standard marine solution at 25 °C (35‰ salinity, Ocean). A. salina nauplii (<72-h old) were exposed to untreated and treated samples for 24 h in quadruplicate to score frequencies of immobilization of 20 nauplii in 2 mL volumes. Negative control with ocean was also performed in parallel according to Migliore *et al.* [25].

Rotifer

A small sample of cysts was obtained from Genetics Department of the NIOF and a rotifer population hatched from these cysts has ever since been in continuous culture at the same Institute. This population has been inbred and selected for cyst production for several generations and consequently is highly homozygous. Cyst hatching is started by transferring the cysts to warmer temperature, lower salinity, and light. Several hundred cysts are placed in 10 ml of seawater medium in a 20 ml dish, which is a convenient size for neonate collection. Procedures for the rotifer acute toxicity bioassay generally follow the recommendations of Standard Methods for the Examination of Water and Wastewater (APHA) [26].

Vibrio parahaemolyticus

The bacteria were cultured in nutrient Agar medium for 16 hrs. The antibacterial activity of wastewater and treated water was tested by disc diffusion assay method [27]. *Vibrio parahaemolyticus* was kindly provided by Microbiology Department of the NIOF, Alexandria, Egypt. The Nutrient Agar plates used for antibacterial tests were incubated at 37 °C for 24 h. An inoculums size, 10^6 cfu/mL for bacteria. Antibacterial activity was determined by measuring the diameter of the zone of inhibition (Mean ± SD) surrounding bacterial growth. All tests were triplicated and the average was reported.

RESULTS AND DISCUSSION

X-Ray diffraction measurements

The as-prepared pure sample showed (101), (004), (200), (100) and 204 peaks at 2θ values of 25.24, 37.32, 47.99, and 53.81°, 62.54 indicating that the as-prepared pure TiO_2 has an anatase crystal structure according to JCPDS-21-1272. XRD of all the doped samples also showed that the peak positions of the obtained anatase structure are shifted slightly towards the left as compared with that of pure anatase TiO_2 (Fig. 1, Table 1). This shift refers to the incorporation of doped ions into the anatase. The crystallite sizes of the specimens were estimated from full-width at half-maximum of the 101 anatase peak by the Debye-Sherrer equation (2) [28,29]

$$C_s = \frac{0.9\lambda}{\beta cos\theta} \quad (2)$$

Where C_s is the crystallite size, β is the full width at half-maximum ($FWHM_{hkl}$) of the more intense peak.

FTIR spectroscopy

The FT-IR spectra of anatase phases TiO_2, C-TiO_2, S-TiO_2 and C,S-TiO_2 NPs samples are shown in Fig. 2. The peaks at 3200-3500 cm^{-1} were assigned to the stretching vibration and bending vibration of surface –OH group and the band at 520-590 observed for all samples was assigned to the Ti-O stretching vibration [30,31], Ti-O-C and Ti-O-S vibration bonds of the C – and S-doped TiO_2 samples emerged at 1060 and 1049 cm^{-1} [32], respectively. These results refer to introducing each of C and S into TiO_2 lattice.

Ultraviolet-visible spectrometry

In order to determine the photo absorbance properties, C-TiO_2, S-TiO_2 and C,S-TiO_2 NPs were analysed by UV-Vis at wavelengths of 200–800 nm (Fig. 3). It's shown that the non-metal doped element shifts the catalyst toward the longer wavelength at the visible region. The band gap (E, eV) of the samples was calculated by using equation (3) [33] as follows:

$$E = \frac{1240}{\lambda_{max}} \quad (3)$$

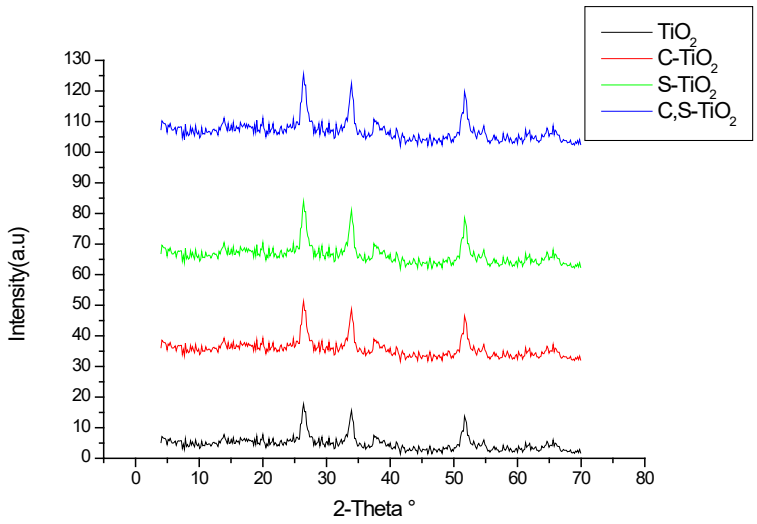

Fig. 1: XRD patterns of TiO_2, C-TiO_2, S-TiO_2 and C,S-TiO_2 NPs.

Table 1. Calculated crystal size of TiO_2, C-TiO_2, S-TiO_2 and C,S-TiO_2 NPs.

TiO_2		C-TiO_2		S- TiO_2		N,S- TiO_2	
Position	Cry Size L (nm)	Position	Cry Size L (nm)	Position	Cry Size L (nm)	Position	Cry Size L (nm)
25.24	30.5	25.22	71.6	25.24	31.0	25.24	30.8
37.32	3.0	37.06	11.1	37.22	36.1	37.22	35.9
37.78	39.6	37.70	92.3	37.70	3.3	37.60	3.0
38.36	3.0	38.36	3.0	47.99	36.2	47.99	36.2
47.99	36.2	47.93	80.1	53.79	21.4	53.79	20.9
53.82	33.8	53.77	89.6	55.00	30.4	55.00	30.1
62.54	26.3	62.77	50.8	62.58	20.6	62.58	20.2

where λ_{max} is the wave length at the maximum absorption. The calculated band gap for C-TiO_2, S-TiO_2 and C,S-TiO_2 NPs are 2.91, 2.70 and 2.80, respectively.

Energy-dispersive X-ray spectroscopy

EDAX spectroscopy confirmed the presence of an elemental titanium, oxygen, sulphur and carbon signals of nanoparticles. The results obtained confirmed the presence of titanium, oxygen, carbon and sulphur elements in the range 4–5, 0.5, 0.3 and 2-2.3 keV, respectively (Fig. 4).

Scanning electron micrographs

The surface morphological study of the C-TiO_2, S-TiO_2, C,S-TiO_2 photocatalysts was carried out using SEM. Fig. 5 shows the SEM image of the TiO_2, C-TiO_2, S-TiO_2 and C,S-TiO_2 NPs, respectively. It can be seen that the shape of the NPs differs slightly by changing the type of dopant material.

Photocatalytic activity

The photocatalytic activities of the studied samples were evaluated by measuring the photocatalytic degradation of RB-19 and RR-76 aqueous solutions under visible light irradiation. The % degradation efficiency (η) for each of pure and doped TiO_2 samples was computed using the following equation (4):

$$\eta = \frac{(A_0 - A_t)}{A_0} \times 100\% \quad (4)$$

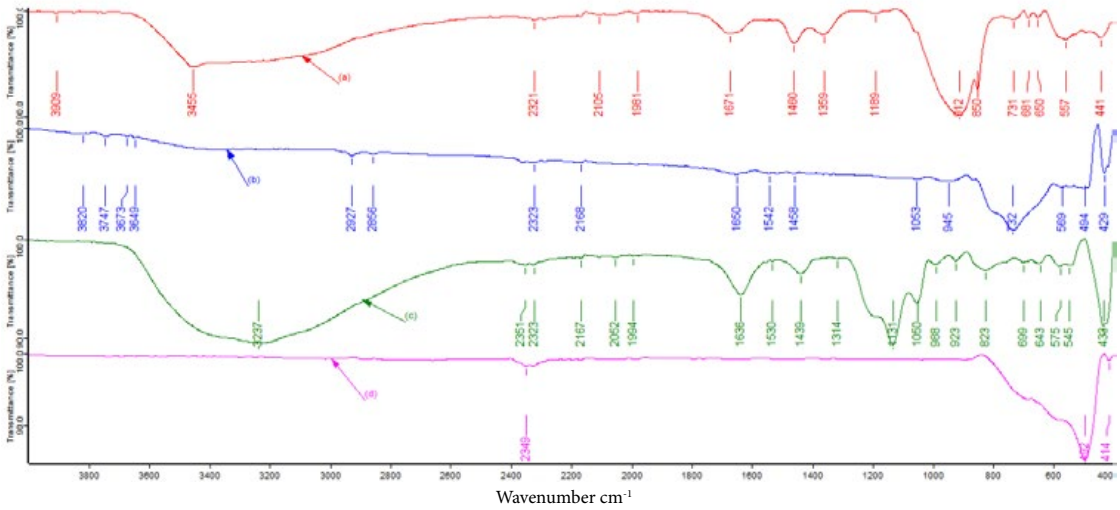

Fig. 2: FT-IR spectra of anatase (a) TiO_2, (b) C-TiO_2, (c) S-TiO_2 and (d) C,S-TiO_2 NPs.

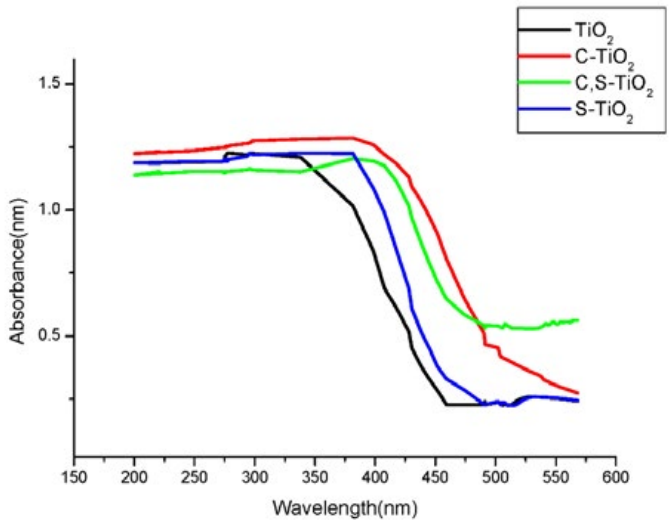

Fig. 3. UV–visible absorption profiles of TiO_2, C-TiO_2, S-TiO_2 and C,S-TiO_2 NPs.

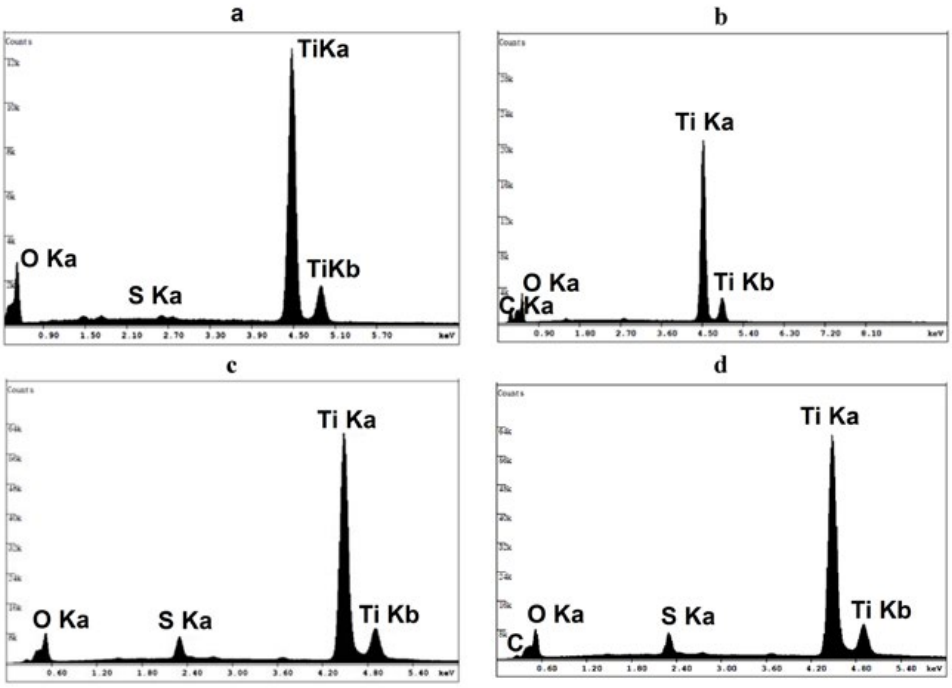

Fig. 4. EDAX of anatase (a) TiO_2, (b) C-TiO_2, (c) S-TiO_2 and (d) C,S-TiO_2 NPs.

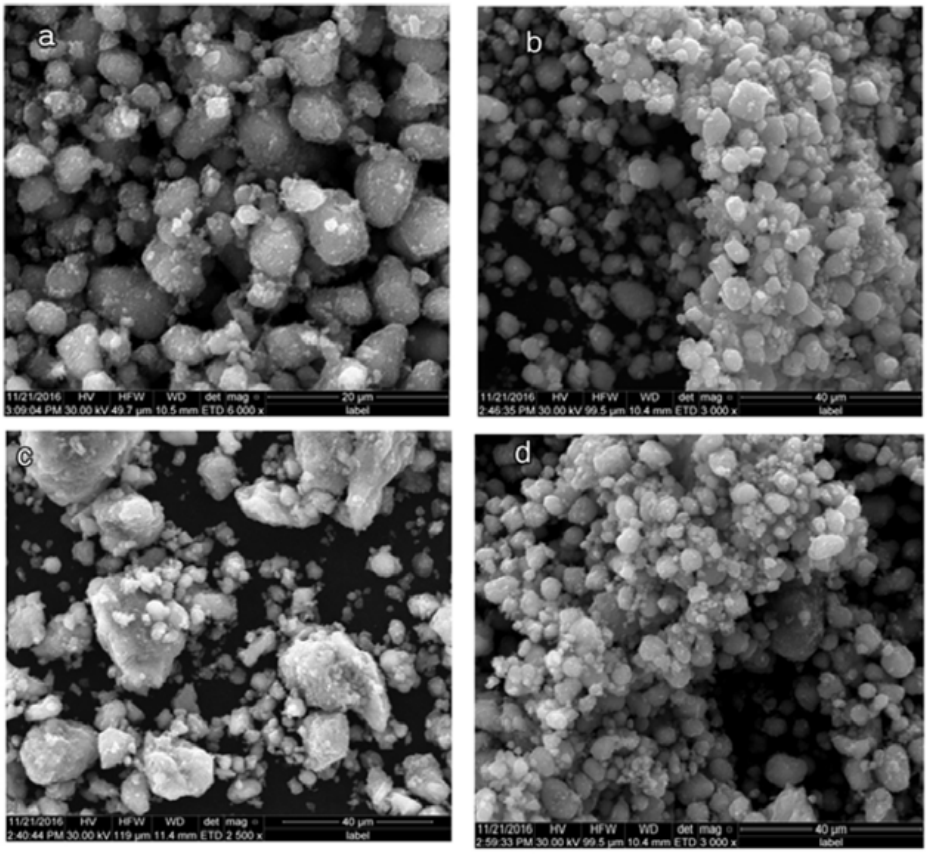

Fig. 5: SEM of anatase (a) TiO_2, (b) C-TiO_2, (c) S-TiO_2 and (d) C,S-TiO_2 NPs.

Where A_0 and A_t are the absorption intensities of dyes at the beginning and at the time t of the photocatalytic degradation reaction. Photocatalytic performance of anatase TiO_2 is greatly improved with the dopant ions. The different activity degrees of the catalysts for both dyes show that the photocatalytic activity of samples effectively depended on the dopant type used. For economic removal of pollutants from the industrial wastewater, it is very important to find the optimum conditions for efficient photocatalytic degradation. Therefore, we studied each of pH, catalyst dosage, dye concentration, shaking speed and irradiation time effects on the degradation rate of photocatalytic reaction. The concentrations of organic dyes present in industrial wastewater were calculated from calibration curves for RR-76 and RB-19, respectively.

Effect of irradiation time

The irradiation time was studied in the range of 0 - 120 min under the light source by loading 0.08 mg of photocatalyst into 50 ml of wastewater that has pH 1. The results obtained are shown in Fig. 6 and summarized in Table 2. They showed an increase in the degradation efficiency by introducing the doping elements into TiO_2 lattice, especially for the samples containing sulphur. Moreover, for all doped samples the degradation efficiency reach 100% in two hours under visible light for both dyes investigated.

Effect of pH

Since photocatalysis occurs at the surface, therefore the effect of pH on the degradation rate of RB-19 and RR-76 using the pure and doped TiO_2 samples was investigated in the pH range 1.0 to 13.0. The interpretation of the pH effect on the degradation process is difficult as it contains various factors such as electrostatic interactions between the catalyst surface and reaction of charged radicals such as superoxide, hydroxyl radicals, etc. moulded on the catalyst surface with pollutant molecules. The

Table 2: Photocatalytic degradation efficiency (η) of RB-19 and RR-76 dyes using C-TiO_2, S-TiO_2, C,S-TiO_2 NPs at different irradiation time, pH, catalyst load, organic substrate concentrations, shaking speeds and effect of regeneration times on the degradation efficiency.

Parameters	Variables	TiO_2 (η)		C-TiO_2 (η)		S-TiO_2 (η)		C,S-TiO_2 (η)	
		RB-19	RR-76	RB-19	RR-76	RB-19	RR-76	RB-19	RR-76
Irradiation time (min)	15	0.0	0.0	53.8	74.0	71.4	61.3	77.8	54.4
	30	2.8	5.0	87.5	87.1	77.8	72.4	92.0	72.5
	60	8.3	11.3	100.0	100.0	84.6	78.6	100.0	79.6
	120	11.1	16.3	100.0	100.0	100.0	100.0	100.0	100.0
pH	1	16.7	18.8	100.0	100.0	92.0	100.0	100.0	100.0
	3	13.9	13.8	67.9	86.2	54.8	85.2	60.0	69.2
	5	11.1	11.3	44.6	42.1	41.2	66.7	50.0	51.7
	7	8.3	8.8	40.3	17.4	17.1	61.3	29.7	15.8
	9	5.6	6.3	34.3	12.5	14.3	51.5	17.1	12.8
	11	2.8	3.8	56.7	38.5	4.3	38.9	4.3	8.6
	13	2.8	1.3	54.1	74.2	4.3	25.0	4.3	6.0
Catalyst dose (g/50 ml)	0.01	2.8	6.3	11.4	16.3	9.1	61.3	4.3	6.0
	0.02	5.6	11.3	37.6	42.9	26.3	78.6	17.1	25.7
	0.04	11.1	13.8	42.7	49.3	65.5	85.2	29.7	60
	0.08	13.9	18.8	51.9	69.5	65.5	100	50	79.6
	0.16	16.7	18.8	98.3	100	100	100	100	100
Dilution ratio	1:0	16.7	18.8	71.4	54.0	17.1	61.3	37.1	79.6
	1:1	22.2	31.3	87.5	77.6	50.0	78.6	50.0	87.2
	1:2	27.8	36.3	100	83.2	71.4	92.3	84.6	95.6
	1:4	44.4	48.8	100	100	100	100	100	100
Shaking speed (rpm)	50	0.0	13.8	87.5	55.4	71.4	61.3	20.5	20.0
	100	2.8	17.5	100.0	61.1	77.8	72.4	29.4	50.0
	150	11.1	18.8	100.0	74.0	84.6	78.6	91.3	100.0
	200	16.7	18.8	100.0	100.0	100.0	100.0	100.0	100.0
	250	16.7	18.8	100.0	100.0	100.0	100.0	100.0	100.0
Cycle times For regeneration	1	16.7	18.8	100.0	100.0	100.0	100.0	100.0	100.0
	2	16.7	18.8	100.0	100.0	100.0	100.0	100.0	100.0
	3	16.0	18.6	100.0	100.0	100.0	100.0	100.0	100.0
	4	16.0	18.5	97.0	96.0	95.0	94.0	96.0	95.0
	5	15.5	17.5	95.0	94.0	93.0	92.0	94.0	93.0

results are represented in Fig. 6 and summarized in Table 2. It can be seen that on decreasing pH of wastewater, the degradation efficiency increases to reach 100% at pH 1 for both RB-19 and RR-76 for all used catalyst except for S-TiO_2 sample, which reaches 92% for RB-19. Also the degradation increases by increasing pH for all used catalyst except for C-TiO_2 which showed a minimum at pH 9 with degradation efficiencies 30.2% and 12.5% for RB-19 and RR-76, respectively. The difference in degredation results can be attributed to the different in type of used catalyst. The pH range has an important role, since it starts the photodegradation process, by initiating the photolysis process of the used catalyst solution, which produces the very reactive OH radical that is responsible for attacking the pollutant to start degradation process. The data indicates that the photocatalytic degradation process was effective in acidic environment.

Effect of photocatalyst load

To find the optimum amount of photocatalyst load for efficient degradation, the wastewater degradation efficiency was studied by varying the amount of photocatalyst load from (0.010 to 0.16 g/50 ml of wastewater) at pH 1 for 2 h. The results obtained are illustrated in Fig. 7(a, b) and Table 2. They show an increase in the photocatalytic degradation efficiency with increasing the amount of photocatalyst.

Effect of organic substrate concentration

The textile wastewater commonly contains organic dyes, inorganic salts and others. Higher concentrations of inorganic salts load in the wastewater can slow down the degradation of organic dyes in the wastewater. The effect of dye concentration on the photocatalyst degradation efficiency of RB-19 and RR-76 dyes was studied by the dilution of raw wastewater that has concentrations of 4.49 ppm of RR-76 and 6.10 ppm of RB-19 in different dilution ratios (1:0, 1:1, 1:2 and 1:4). Fig. 7(c, d) and Table 2 show the effect of concentration of dyes in the wastewater on the degradation efficiency. For all photocatalysts and both dyes investigated, the degradation was found to decrease with increasing the dye concentration, i.e. the degradation efficiency was very low when the raw wastewater was subjected to photodegradation without dilution. This is due to scattering of light by higher concentration of organic substrate and less transmission of light through the wastewater.

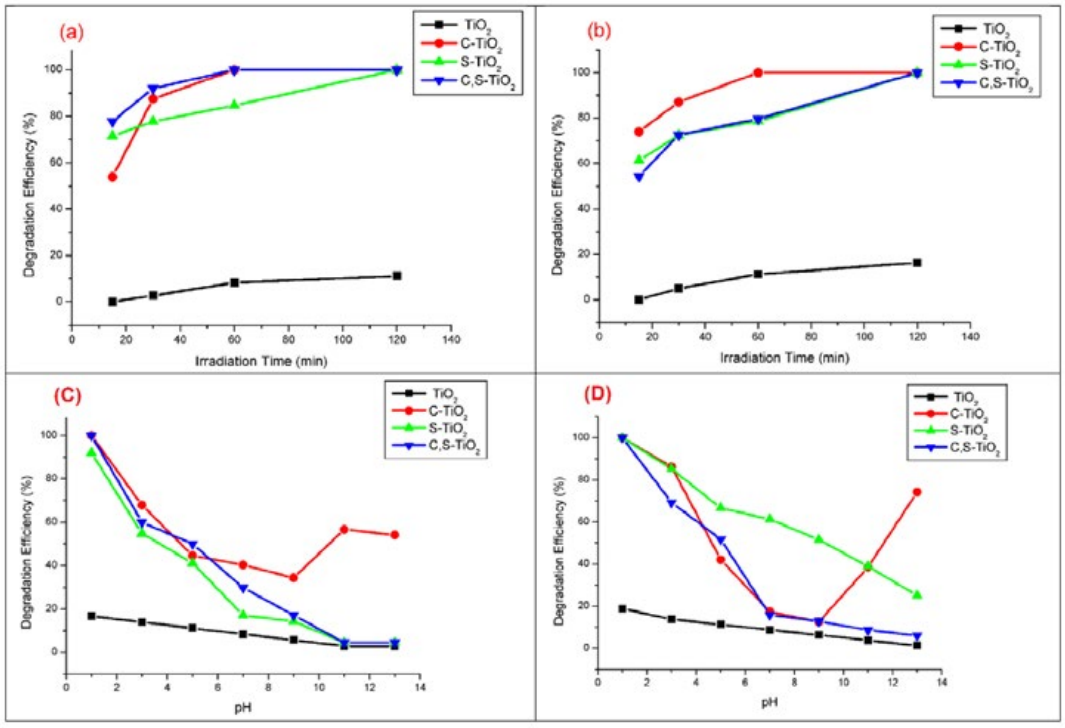

Fig. 6: Effect of irradiation time on RB-19 (a) and RR-76 (b) and pH on RB-19 (c) and of RR-76 (D) using the photocatalytic degradation efficiency present in industrial wastewater using TiO_2, C-TiO_2, S-TiO_2 and C,S-TiO_2 NPs photocatalysts.

Effect of shaking speed

The effect of shaking speed on the degradation of dyes in the wastewater was studied under visible light source with continuous shaking in the photoreactor using shaking incubator with different shaking speed (50-250 rpm). The continuous shaking causes homogeneous distribution of photocatalysts in the solution and also increases the solution flow along the photocatalysts surfaces. Another set of photocatalytic experiments were carried out without stirring and all other experimental parameters were kept constant in all the experiment runs. Fig. 8(a, b) show the effect of shaking mechanism on the photocatalytic degradation efficiency under visible light source (Table 2). The degradation efficiency using photocatalyst considerably increased with increaing shaking speed. Shaking creates localized turbulence near the base of the photocatalyst and enhances the mixing of organic substrate in the wastewater and it brings the organic pollutants into contact with photocatalysts in the aqueous solution and decreases the boundary layer distance leading to an increase in the degradation efficiency of organic pollutants in the aqueous medium. Degradation efficiency was found to be higher by using C-doped TiO_2 and C,S co-doped TiO_2 than that by using S-doped TiO_2 sample.

Catalyst recovery

In the present, the recovery of the suspended photocatalyst was easily achieved by filtration using 0.45 µm cellulose acetate filter paper, washing with water and ethanol several times then by drying in oven at 80-100 °C. The recovered catalysts were used repeatedly more than 3 times without significant decrease of its activity (Table 2 and Fig. 8c, d).

Detoxification of industrial textile wastewater

The acute toxicity of treated and untreated textile wastewater was determined by using rotifer. The results obtained showed that untreated wastewater exhibits very high toxicity on rotifer (more than 85% toxicity), while treated solution displayed very slight toxicity (less than 15% of cell growth inhibition) in respect to changing pH of treated solution till it reaches a value between 7 and 8 before putting it into source of drain water, while the pH of wastewater after treatment ranged from 1.30-2.5 which will have a negative effect on rotifer and artemia that prefer neutral medium. The toxicity of the samples tested on rotifer and artemia salina are about 95-98% for untreated and very slight toxicity (less than 5%) for treated ones with special

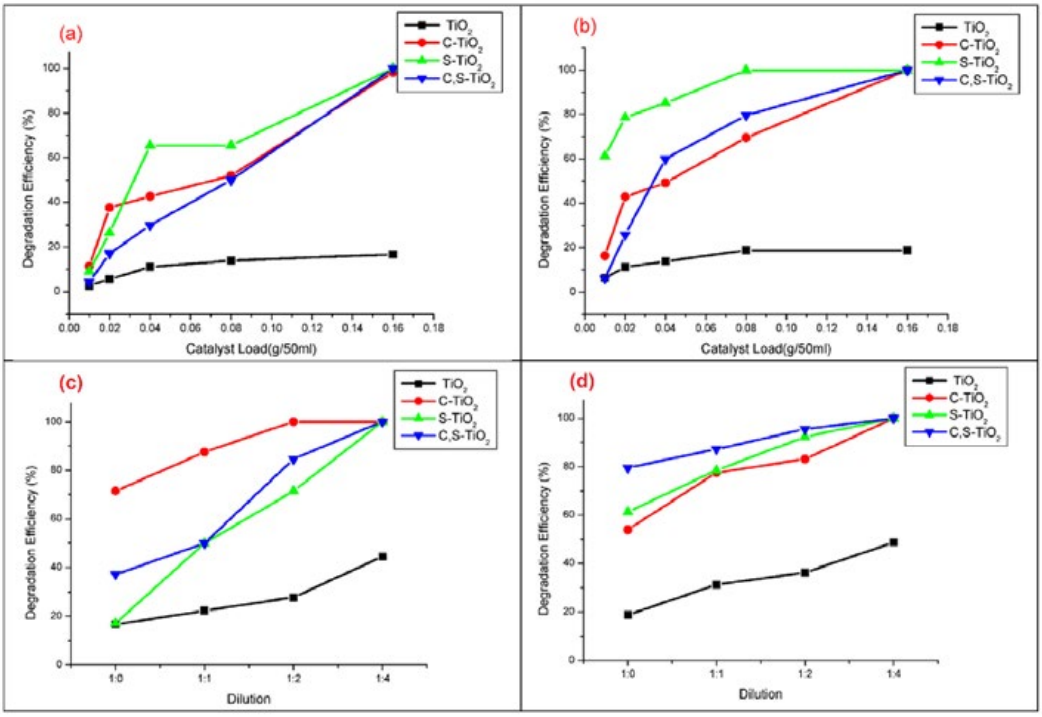

Fig. 7: Effect of photocatalyst load RB-19 (a) and of RR-76 (b) and Effect of organic matter concentration in wastewater RB-19 (c) and of RR-76 (d) on the degradation efficiency of present in industrial wastewater using TiO_2, C-TiO_2, S-TiO_2 and C,S-TiO_2 NPs as photocatalysts

precaution taken for artemia. Fig. 9 shows rotifer and artemia under microscope before and after being exposed to treated and untreated industrial wastewater. The organisms are immobilized after being exposed to untreated wastewater, while speed of about (5%) was slightly decreased after being exposing to treated wastewater**.** The antibacterial activity of wastewater and treated wastewater was examined against *Vibrio parahaemolyticus*. In this study, the treated wastewater using S-TiO_2 showed the highest activity against *Vibrio parahaemolyticus*. The activity of treated wastewater using different photocatalysts follows the following order S-TiO_2 NPs > C,S-TiO_2 NPs > C-TiO_2 NPs. These results indicate that treated wastewater has antibacterial activities against tested microorganisms (*Vibrio parahaemolyticus*) with inhibition zone 18.5±0.3, 21.5±0.3, 25.2±0.2 and 20±0.3 for TiO_2, C-TiO_2, S-TiO_2 and C,S-TiO_2NPs, respectively.

Chemical oxygen demand

COD test used for indirectly determination of the organic pollutants amount found in wastewater, making it a useful tool for measuring quality of water, which measures the mass of consumed oxygen per liter of solution. The measured COD values for treated and untreated wastewater are 40, 5.0, 4.5, and 4.3 for wastewater, treated using C-doped TiO_2, S-doped TiO_2 and C,S co-doped TiO_2 NPs, respectively. This indicates that the calculated efficiency for treated wastewater is 87.50, 88.70 and 89.25 using C-doped TiO_2, S-doped TiO_2 and C,S-TiO_2 NPs, respectively. The results indicate that there are some inorganic pollutants as chlorine that may cause interference making COD values different from that calculated using spectrophotometer.

TiO_2 was doped with certain metals, non-metals and ionic components to enhance the process of photo-catalysis [34-37]. Doped ions can also act as charge trapping sites and thus reduce electron–hole recombination [38]. Doping with non-metals such as nitrogen, sulfur, halogens, carbon and boron is commonly used for the band gap modification. An anion sulfur can be doped by substituting oxygen sites of TiO_2 or doped as a cation by replacing Ti^{4+} ions in TiO_2. Band gap of TiO_2 can be reduced by doping with sulfur. Boron enhances TiO_2 absorption of visible light even to 800 nm by shifting the band edge of TiO_2 to higher

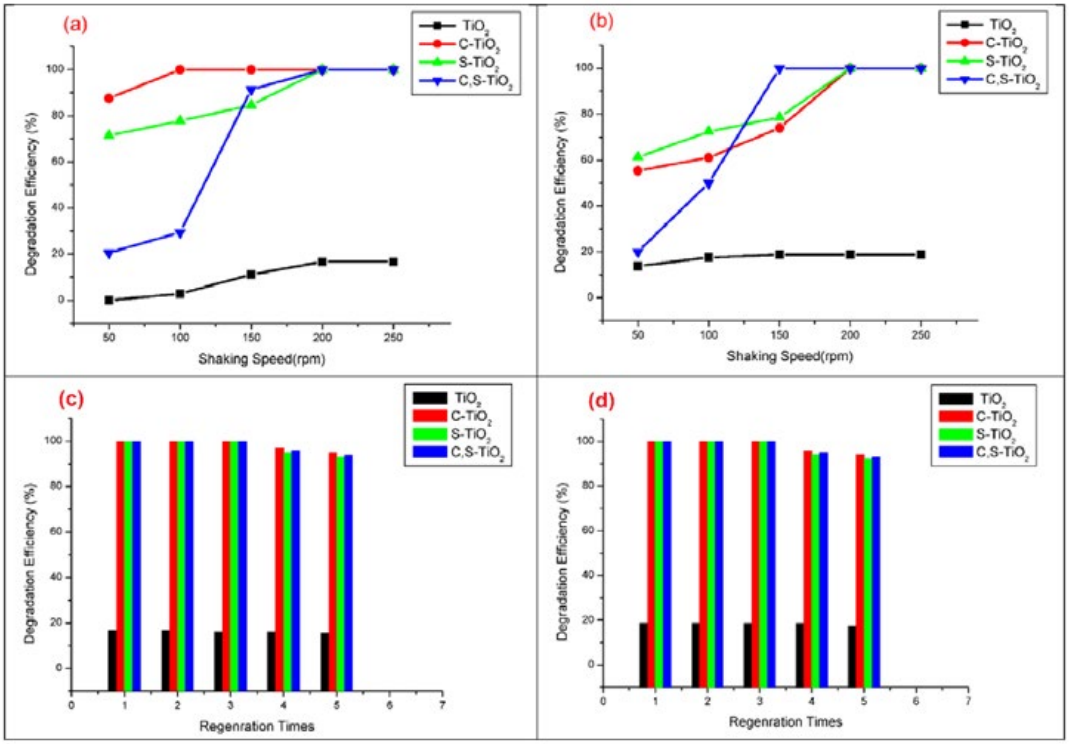

Fig. 8: Effect of shaking speed on the degradation efficiency RB-19 (a) and of RR-76 (b) and effect of regeneration times on the degradation efficiency RB-19 (c) and of RR-76 (d) present in industrial wastewater using TiO_2, C-TiO_2, S-TiO_2 and C,S-TiO_2 NPs as photocatalysts.

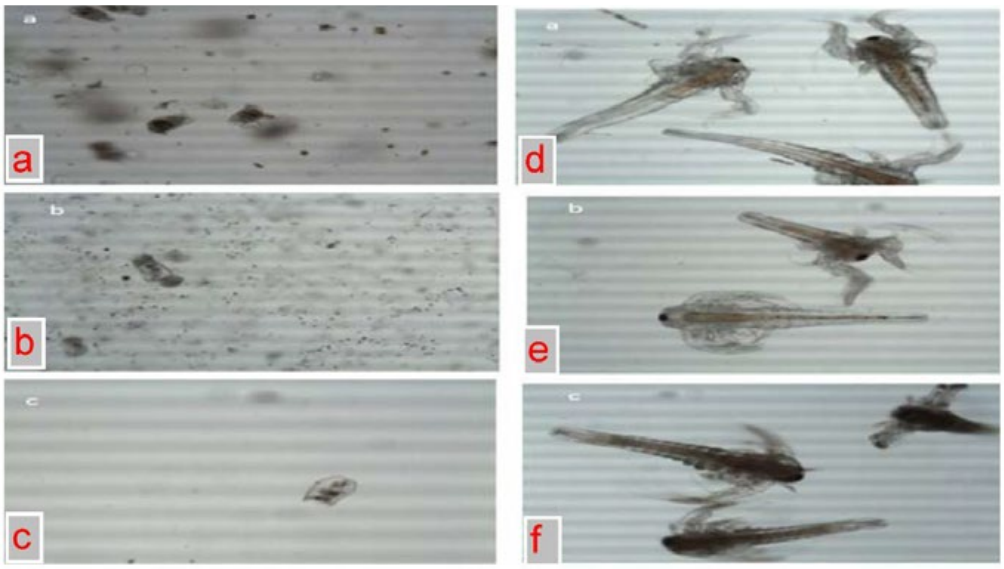

Fig. 9: (a) Rotifer before exposed to wastewater, (b) after exposed to treated wastewater, (c) after exposed to untreated industrial wastewater, and (d) Artemia before exposed to wastewater, (e) after exposed to treated wastewater and (f) after exposed to untreated industrial wastewater.

wavelengths. Boron can substitutes the O sites in TiO_2 lattice. Carbon has been incorporated in TiO_2 lattice both as an anion and as a cation that reducing the band gap value. Co-doping with non-metals has been also tested reaching higher hydrophilicity [37]. The dye degradation efficiency decreases by further increasing the dye concentration because the dye ions may cover the active sites at high concentrations of dye and therefore decreases the generation of radicals on the surface. Another reason is the light-screening effect of the dye itself [38-39]. The intermediate products formed by the dye degradation increased by increasing the initial dye concentration lead to require more time to complete the degradation process [39]

CONCLUSION

TiO_2, C-doped TiO_2, S-doped TiO_2 and C,S co-doped TiO_2 NPs were prepared by sol-gel method and the structure and morphology were characterized using different techniques. These photocatalysts possess the highest visible light absorption. The degradation of RB-19 and RR-76 organic dyes pollutants present in the industrial wastewater under visible light range were investigated under several experimental parameters such as pH, catalyst load, and organic concentration, irradiation time, shaking speed and catalyst recovery. The degradation efficiency of wastewater containing dyes exhibits the highest value under pH of 1 and almost 1 h. This study provides a versatile approach for highly efficiency method for the degradation of textile wastewater pollutants under solar irradiation in the presence of C-doped TiO_2, S-doped TiO_2 and C,S co-doped TiO_2 NPs photocatalyst. The treated wastewater doesn't possesse toxicity against rotifer and artemia marine organisms.

CONFLICT OF INTEREST

The authors declare that there are no conflicts of interest regarding the publication of this manuscript.

REFERENCES

1. El Nemr A. Impact, Monitoring and Management of Environmental Pollution, 1st edited, Nova Science Publishers, USA (2010), ISBN: ISBN-10: 1608764877, ISBN-13: 9781608764877.
2. El Nemr A, Non-Conventional textile waste water treatment, 1st edited, Nova Science Publishers, USA, 2012, ISBN: 978-1-62100-079-2; 978-1-62100-228-4.
3. El Nemr A, Textiles: Types, Uses and Production Methods, 1st edited by Ahmed El Nemr, Nova Science Publishers, USA, 2012, ISBN: 978-1-62100-239-0; 978-1-62100-284-0.
4. Houas A. Photocatalytic degradation pathway of methylene blue in water. Applied Catalysis B: Environmental. 2001;31(2):145-57.
5. Arami M, Limaee N, Mahmoodi N, Tabrizi N. Equilibrium and kinetics studies for the adsorption of direct and acid dyes from aqueous solution by soy meal hull. Journal of Hazardous Materials. 2006;135(1-3):171-9.
6. Yang W, Wu D, Fu R. Effect of surface chemistry on the adsorption of basic dyes on carbon aerogels. Colloids and

Surfaces A: Physicochemical and Engineering Aspects. 2008;312(2-3):118-24.
7. Ruan S, Wu F, Zhang T, Gao W, Xu B, Zhao M, Photodegradation of dyes by a novel TiO2/u-RuO2/GNS nanocatalyst derived from Ru/GNS after its use as a catalyst in the aerial oxidation of primary alcohols (GNS = graphene nanosheets), Mater. Chem. Phys. 2001:69-70.
8. Al-Qaradawi S, Salman SR, Photocatalytic degradation of methyl orange as a model compound, J. Photochem. Photobiol. A: Chem. 2002:148-161.
9. Jia B-Y, Duan L-Y, Ma C-L, Wang C-M. Characterization of TiO2 Loaded on Activated Carbon Fibers and Its Photocatalytic Reactivity. Chinese Journal of Chemistry. 2007;25(4):553-7.
10. Asilturk M, Sayilkan F, Erdemoglu S, Akarsu M, Sayilkan H, Erdemoglu M, et al. Characterization of the hydrothermally synthesized nano-TiO2 crystallite and the photocatalytic degradation of Rhodamine B. Journal of Hazardous Materials. 2006;129(1-3):164-70.
11. Wilhelm P, Stephan D. Photodegradation of rhodamine B in aqueous solution via SiO2@TiO2 nano-spheres. Journal of Photochemistry and Photobiology A: Chemistry. 2007;185(1):19-25.
12. Kim DS, Park YS. Photocatalytic decolorization of rhodamine B by immobilized TiO2 onto silicone sealant. Chemical Engineering Journal. 2006;116(2):133-7.
13. Li Y, Sun S, Ma M, Ouyang Y, Yan W. Kinetic study and model of the photocatalytic degradation of rhodamine B (RhB) by a TiO2-coated activated carbon catalyst: Effects of initial RhB content, light intensity and TiO2 content in the catalyst. Chemical Engineering Journal. 2008;142(2):147-55.
14. Khan SB, Hou M, Shuang S, Zhang Z. Morphological influence of TiO 2 nanostructures (nanozigzag, nanohelics and nanorod) on photocatalytic degradation of organic dyes. Applied Surface Science. 2017;400:184-93.
15. Huang J, Song H, Chen C, Yang Y, Xu N, Ji X, et al. Facile synthesis of N-doped TiO 2 nanoparticles caged in MIL-100(Fe) for photocatalytic degradation of organic dyes under visible light irradiation. Journal of Environmental Chemical Engineering. 2017;5(3):2579-85.
16. Alamelu K, Raja V, Shiamala L, Jaffar Ali BM. Biphasic TiO 2 nanoparticles decorated graphene nanosheets for visible light driven photocatalytic degradation of organic dyes. Applied Surface Science. 2018;430:145-54.
17. Chen F, Yang X, Mak HKC, Chan DWT. Photocatalytic oxidation for antimicrobial control in built environment: A brief literature overview. Building and Environment. 2010;45(8):1747-54.
18. Gomathi Devi L, Narasimha Murthy B, Girish Kumar S. Heterogeneous photo catalytic degradation of anionic and cationic dyes over TiO2 and TiO2 doped with Mo6+ ions under solar light: Correlation of dye structure and its adsorptive tendency on the degradation rate. Chemosphere. 2009;76(8):1163-6.
19. Kim DS, Kwak S-Y. Photocatalytic Inactivation ofE. coliwith a Mesoporous TiO2Coated Film Using the Film Adhesion Method. Environmental Science & Technology. 2009;43(1):148-51.
20. El Nemr A, Hassaan MA, Madkour FF, HPLC-MS/MS Mechanistic study of Direct Yellow 12 dye degradation using Ultraviolet assisted ozone process, J. Water Environ. Nanotech. 2018; 3(1):1-11.
21. Hassaan MA, El Nemr A, Madkour FF. Testing the advanced oxidation processes on the degradation of Direct Blue 86 dye in wastewater. The Egyptian Journal of Aquatic Research. 2017;43(1):11-9.
22. Hassaan MA, El Nemr A, Madkour FF. Advanced oxidation processes of Mordant Violet 40 dye in freshwater and seawater. The Egyptian Journal of Aquatic Research. 2017;43(1):1-9.
23. Zhang H, Banfield JF. Understanding Polymorphic Phase Transformation Behavior during Growth of Nanocrystalline Aggregates: Insights from TiO2. The Journal of Physical Chemistry B. 2000;104(15):3481-7.
24. Methods for Measuring the Acute Toxicity of Effluents and Receiving Waters to Freshwater and Marine Organisms, Fifth Edition; 2002.
25. Migliore L, Civitareale C, Brambilla G, Delupis GDD. Toxicity of several important agricultural antibiotics to Artemia. Water Research. 1997;31(7):1801-6.
26. Standard Methods for the Examination of Water and Wastewater. 16th Edition, American Public Health Association, Washington DC. 1985.
27. Vander BDA, Vlietnck AJ, Screening methods for antibacterial and antiviral agents from higher plants. In: Dey PM, Harborne JB, Hostiettman K. (eds.) Methods in plant biochemistry. London: Academic Press. 1991:47-69.
28. Li Z, Hou B, Xu Y, Wu D, Sun Y, Hu W, et al. Comparative study of sol–gel-hydrothermal and sol–gel synthesis of titania–silica composite nanoparticles. Journal of Solid State Chemistry. 2005;178(5):1395-405.
29. Cullity BD, Elements of X-Ray Diffraction, Addison-Wesley, Reading, Mass, USA, 1978.
30. Abdullah AM, Al-Thani NJ, Tawbi K, Al-Kandari H. Carbon/nitrogen-doped TiO2: New synthesis route, characterization and application for phenol degradation. Arabian Journal of Chemistry. 2016;9(2):229-37.
31. Yang J, Bai H, Tan X, Lian J. IR and XPS investigation of visible-light photocatalysis—Nitrogen–carbon-doped TiO 2 film. Applied Surface Science. 2006;253(4):1988-94.
32. Li Q, Zhang Z, Zhang K, Xu L, Fang J, Lai Y, et al. Synthesis and electrochemical performance of TiO2–sulfur composite cathode materials for lithium–sulfur batteries. Journal of Solid State Electrochemistry. 2013;17(11):2959-65.
33. Song S, Tu J, He Z, Hong F, Liu W, Chen J. Visible light-driven iodine-doped titanium dioxide nanotubes prepared by hydrothermal process and post-calcination. Applied Catalysis A: General. 2010;378(2):169-74.
34. Ahmed S, Rasul MG, Martens WN, Brown R, Hashib MA. Heterogeneous photocatalytic degradation of phenols in wastewater: A review on current status and developments. Desalination. 2010;261(1-2):3-18.
35. Kassahun SK, Kiflie Z, Shin DW, Park SS. Photocatalytic Decolorization of Methylene Blue by N-doped TiO2 Nanoparticles Prepared Under Different Synthesis parameters. J. Water Environ. Nanotechnol., 2(3);2017:136-144.
36. Nazarpour Laghani S, Ebrahimian Pirbazari A. Photocatalytic Treatment of Synthetic Wastewater Containing 2,4 dichlorophenol by Ternary MWCNTs /Co-TiO2 Nanocomposite Under Visible Light. J. Water Environ. Nanotechnol., 2(4);2017:290-301.37. Rehman S, Ullah R, Butt AM, Gohar ND. Strategies of making TiO2 and ZnO visible light active. Journal of Hazardous Materials. 2009;170(2-3):560-9.
38. Konstantinou IK, Albanis TA. TiO2-assisted photocatalytic degradation of azo dyes in aqueous solution: kinetic and mechanistic investigations. Applied Catalysis B: Environmental. 2004;49(1):1-14.
39. Sabbaghi S, Doraghi F, Photo-Catalytic Degradation of Methylene Blue by ZnO/SnO2 Nanocomposite. J. Water Environ. Nanotechnol. 1(1);2016:27-34.